Eur Radiol (2016) 26:1575–1581
DOI 10.1007/s00330-015-4007-6

BREAST

Contrast-enhanced dual energy mammography with a novel anode/filter combination and artifact reduction: a feasibility study

Thomas Knogler[1,2] · Peter Homolka[4] · Mathias Hörnig[5] · Robert Leithner[4] · Georg Langs[1,3] · Martin Waitzbauer[1,3] · Katja Pinker-Domenig[1,2] · Sabine Leitner[1,2] · Thomas H. Helbich[1,2]

Received: 19 April 2015 / Revised: 27 July 2015 / Accepted: 3 September 2015 / Published online: 15 September 2015

Abstract

Objectives To demonstrate the feasibility of contrast-enhanced dual-energy mammography (CEDEM) using titanium (Ti) filtering at 49 kVp for high-energy images and a novel artefact reducing image-subtraction post-processing algorithm.

Methods Fifteen patients with suspicious findings (ACR BI-RADS 4 and 5) detected with digital mammography (MG) that required biopsy were included. CEDEM examinations were performed on a modified prototype machine. Acquired HE and low-energy raw data images were registered non-rigidly to compensate for possible subtle tissue motion. Subtracted CEDEM images were generated via weighted subtraction, using a fully automatic, locally adjusted tissue thickness-dependent subtraction factor to avoid over-subtraction at the breast border. Two observers evaluated the MG and CEDEM images according to ACR BI-RADS in two reading sessions. Results were correlated with histopathology.

Results Seven patients with benign and eight with malignant findings were included. All malignant lesions showed a strong contrast enhancement. BI-RADS assessment was altered in 66.6 % through the addition of CEDEM, resulting in increased overall accuracy. With CEDEM, additional lesions were depicted and false-positive rate was reduced compared to MG.

Conclusions CEDEM using Ti filtering with 49 kVp for HE exposures is feasible in a clinical setting. The proposed image-processing algorithm has the potential to reduce artefacts and improve CEDEM images.

Key Points

- *CEDEM with a titanium filter is feasible in a clinical setting.*
- *Breast thickness-dependent image subtraction has the potential to improve CEDEM images.*
- *The proposed image-processing algorithm reduces artefacts.*

Keywords Breast cancer · Digital mammography · Contrast-enhanced digital mammography · Image processing · Contrast agent

✉ Thomas Knogler
thomas.helbich@meduniwien.ac.at

[1] Department of Biomedical Imaging and Image-Guided Therapy, Medical University of Vienna, Waehringer Guertel 18-20, 1090 Vienna, Austria

[2] Division of Molecular and Gender Imaging, Medical University of Vienna, Waehringer Guertel 18-20, 1090 Vienna, Austria

[3] Computational Imaging Research Laboratory, Medical University of Vienna, Waehringer Guertel 18-20, 1090 Vienna, Austria

[4] Center for Medical Physics and Biomedical Engineering, Medical University of Vienna, Waehringer Guertel 18-20, 1090 Vienna, Austria

[5] Siemens AG, Healthcare, X-Ray Products, Allee am Röthelheimpark 2, 91052 Erlangen, Germany

Abbreviations

Al	Aluminium
CEDEM	Contrast-enhanced dual-energy mammography
Cu	Copper
FFDM	Full-field digital mammography
HE	High energy
kVp	Kilovolt peak
LE	Low energy
MG	Mammography
Rh	Rhodium
SdNR	Signal-difference-to-noise ratio
Ti	Titanium
W	Tungsten

Introduction

Contrast-enhanced dual-energy mammography (CEDEM) has the potential to improve diagnostic accuracy in lesion detection and characterization through the additional functional information provided by the contrast enhancement of breast tumours [1–7]. CEDEM uses the dual-energy and temporal subtraction technique [2, 8], which takes advantage of characteristic changes in the x-ray attenuation of breast tissue and iodine contrast agent at different photon energies. A high-energy (HE) and a low-energy (LE) image obtained after the administration of an iodinated contrast agent are used for the calculation of a subtraction image with increased conspicuity of the iodine enhancement [8]. CEDEM systems usually use either copper (Cu) [1, 3, 4] or aluminium (Al) [5] as additional filters to further harden the incident photon beam and thus narrow the spectrum to reduce overlap for the HE image exposure, combined with tube potentials between 45 and 49 kilovolt peak (kVp).

In general for beam hardening any material without a K or L edge in the spectral range can be used. Therefore another suitable option for filter material is titanium (Ti). Ti has a relatively low atomic number and therefore absorption edges in the applied spectral energy range can be avoided. The lower atomic number of Ti (Z=22) compared to Cu (Z=29) is further beneficial as there is a larger contribution of the photoelectric effect. Additionally the use of a Ti filter leads to (a) a lower tube load, and (b) a higher signal-difference-to-noise ratio (SdNR) of the iodine enhancement in breast tissue that is apparent in the subtracted image [9]. The SdNR is a measure of the detectability of an object in an x-ray image [10]. It is defined as the ratio between the mean signal difference of the object of interest and the background divided by the standard deviation of the noise in the background [11]. A higher SdNR results in a better visibility of iodine against the structured breast background. SdNR can also be increased through elevated tube voltages, reflecting a greater distance to the K-edge of iodine at 33.2 kV [12, 13].

The application of an intelligent algorithm in the image subtraction process [14], which takes the breast contour into account, avoids subtraction artefacts and increases image quality [6].

The purpose of the study was to evaluate the feasibility of a CEDEM system, using a Ti filter at a fixed tube voltage of 49 kVp for HE images, and to introduce a novel post-processing algorithm for the subtraction process.

Materials and methods

Siemens Healthcare (Erlangen, Germany) provided the equipment for this study. The authors had complete control of the data and the article submitted for publication. Institutional review board approval and written, informed consent from patients were obtained.

Patients

Within a 9-month period, patients who were recalled after screening mammography (MG) and had a suspicious imaging finding at assessment (American College of Radiology (ACR) Breast Imaging Reporting and Data System (BI-RADS) 4 and 5) were offered enrolment in this study. Patients who were pregnant, lactating, younger than 40 years, or had breast implants, prior breast surgery or mastectomy, renal insufficiency, or contraindications to iodinated contrast agent were excluded. Examinations were scheduled between the seventh and 14th day of the menstrual cycle.

Image acquisition

CEDEM was performed with a modified Siemens Mammomat Inspiration full-field digital mammography (FFDM) unit (Siemens Healthcare). For CEDEM a pair of HE and LE images were obtained consecutively during a single breast compression. HE images were obtained with an additional Ti filter. Simulations have verified a tube current lower by a factor of 1.6 for the Ti filter (1 mm) compared to a Cu filter (0.3 mm) as used in other systems, resulting in a lower tube load, for equal image quality [9]. Deterministic simulations were performed with a tungsten (W) anode, different filter materials (rhodium (Rh), Al, Cu, Ti) and thicknesses as well as tube voltages. Breast thicknesses were modified between 20 mm and 80 mm with an assumed 50/50 glandular/fatty tissue fraction. SdNR was computed for a 0.1 mm homogenous iodine slice. Phantom tests were performed using these settings in a CIRS model 020 (CIRS, Virginia, USA), and resulted in 30 % of the dose used for the HE images compared to standard mammograms [9]. As a result, HE images were acquired with a W anode and a 1-mm Ti filter at a fixed tube voltage of 49 kVp. Ti was chosen because of its relatively low atomic number and, thus, absence of absorption edges in the spectral energy range applied. The material thickness chosen represents a compromise between optimum hardening and tube output (tube current). In order to prevent a dose increase due to the iodine contrast, manual exposure technique was used for HE acquisitions. A lookup table was created based on the average glandular dose (AGD) for the LE images acquired with automatic exposure control (AEC) using a CIRS model 020 (CIRS, Virginia, United States) phantom with 50/50 glandular/fatty tissue fraction with different thicknesses (20–80 mm). The AGD of HE was set to approximately 30 % of the AGD for LE. LE images were acquired with a W anode target and a 55-μm Rh filter at a tube voltage of 28–32 kVp according to regular MG imaging protocols, applying the photon energies well below the K-edge of iodine. Exposures were taken in an automatic image acquisition technique using an anti-scatter grid.

Contrast agent administration

Intravenous injection (20-gauge catheter) of contrast agent was performed prior to positioning and breast compression with the patient in a seated position. Breast positioning was equal to conventional mammograms. A single dose of 2 ml/kg body weight of non-ionic iodine contrast media (Iomeron 400, Bracco, Italy) was administered at a rate of 3.5 ml/s using a power injector (Ulrich Medical, Ulm, Germany), followed by a saline flush of 25 ml. Sixty to 90 seconds after administration of the contrast agent, the breast was compressed with standard compression force and imaging began, so that the early-phase enhancement of breast lesions was reached [15]. HE images, which carry mainly the iodine information, were performed first to maximize the dual-energy contrast [16]. LE images were performed after a delay of 30 s. During this time, the HE image was displayed, and filters were changed and moved into the x-ray beam automatically. In this prototype setting only one view was acquired; however, we are aware that in a clinical setting two views are mandatory [3].

Image processing

Image reconstruction software was written in Matlab (MathWorks, Ismaning, Germany) and included two steps. First, LE and HE images were registered non-rigidly to compensate for possible subtle tissue motion between the two images (Fig. 1) [17]. Then a weighted subtraction of the logarithmic images was performed according to:

$$CEDEM = \ln HE - \mathrm{w}(s,t) * \ln LE$$

The corresponding weighting factor, w(s,t), is optimized to cancel background breast tissue, resulting in minimal anatomical noise. In order to maximize the augmentation of the iodine contrast and minimize anatomical noise, w(s,t) is dependent on the x-ray spectra used (s), and the compressed breast thickness (t), accounting for both individual differences, as well as decreasing tissue thickness toward the periphery of the organ. Therefore the breast contour is detected using a segmentation algorithm. Local breast thickness in the border region is then estimated by applying spline interpolation and a geometric model of the compressed breast tissue. The resulting w(s,t) in the subtraction then becomes locally dependent on the tissue thickness estimate, resulting in high values in the centre and gradually lower values in the margin area [18]. This approach is superior to a constant w(s,t), since the latter would result in over-subtraction at the border that might conceal contrast-enhancing lesions at the breast margin (Fig. 2). To determine the optimal w(s,t) an image entropy minimization algorithm is applied, since subtracted images with less anatomical noise, i.e. better cancellation of non-iodine-related structures, are mathematically related to a lower image entropy. All images were stored digitally.

Image evaluation

In addition to the CEDEM image, full-field digital mammography (FFDM) images were available for all patients. Diagnosis was established via core-needle biopsy and/or surgery in all patients [19]. In case of additional lesions detected with CEDEM that were not visible with FFDM, e.g. multifocal or multicentric cancers, additional magnetic resonance imaging (MRI) was performed. Additional lesions underwent either MR-guided or ultrasound-guided biopsy if visible on second-look ultrasound. All images were evaluated independently by two radiologists (Readers 1 and 2) with more than 6 years of experience in breast imaging. In case of a discrepancy, the final decision was made in consensus. Evaluation was performed on a Syngo® MammoReport workstation (Siemens) under slightly increased ambient light settings [20].

Readers were blinded to inclusion criteria, clinical information, patient history and previous MGs. Images were anonymised and shown in a random order in two independent sessions. In the first session, the set of MGs (two views) were reviewed. Thirty days after the first session, the MGs and the CEDEM images were evaluated side by side. In case of a discrepancy in the final BI-RADS assessment between the MG and CEDEM, the results of the CEDEM were always used for the final BI-RADS classification. This could result in an up- or downgrading of the initial MG BI-RADS classification. MGs and subtracted CEDEM images were reviewed based on the criteria from the BI-RADS lexicon [21]. For the interpretation of the subtracted CEDEM images, criteria on contrast enhancement intensity and morphology were adopted from the MRI part of the BI-RADS lexicon [21]. Subjective judgement of lesion enhancement was based on a four-option scale, i.e. strong, moderate, weak and none.

Results

Seven benign and eight malignant lesions were found in 15 patients (median age, 58 years; range, 44–74 years). Table 1 summarizes the details for each patient and the results of the image evaluation. Of the eight patients with malignant lesions, five had a single lesion, one had a multifocal cancer with four lesions (patient 9) and two had multicentric cancer with three lesions (patient 10) and five lesions (patient 14). In the multifocal and multicentric lesions CEDEM depicted three (patient 9), two (patient 10) and four (patient 14) additional lesions that were not visible in FFDM. All malignant lesions showed a strong contrast enhancement at CEDEM. Moderate enhancement was seen in two benign lesions. The remaining benign lesions showed no enhancement.

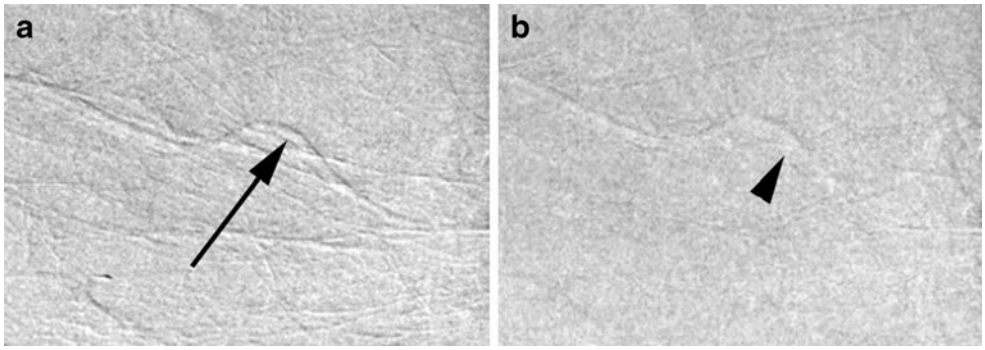

Fig. 1 Effect of non-rigid co-registration of low energy (LE) and high energy (HE) images on the subtracted contrast-enhanced dual-energy mammography (CEDEM) image. Breast structures are surrounded by a thin black shadow in non-registered CEDEM images due to subtle tissue motion between the acquisition of LE and HE images, e.g., vessels (arrow in **a**). No shadows are visible after applying co-registration, and the subtracted CEDEM image appears more homogenous (arrowhead in **b**)

Through the combination of the MG and CEDEM, BI-RADS assessment changed in 10/15 (66.6 %) patients. In five cases (33 %), BI-RADS was upgraded from BI-RADS 4 to 5. In two cases (13 %), BI-RADS was downgraded from BI-RADS 4 to 2 (Fig. 3), in two cases (13 %) from BI-RADS 3 to 2, and in one case (7 %) from BI-RADS 4 to 1.

Discussion

The results of our study show that the CEDEM system studied, using a Ti filtering of 1-mm thickness to harden the 49 kVp W-anode X-ray spectra for HE acquisition, generated images that are clinically useful. This method, combined with a subtraction algorithm to account for local breast tissue thickness, especially in the border region of the compressed breast, is feasible. It allowed the analysis of breast lesions with a high diagnostic accuracy.

Several studies have shown the potential value of CEDEM for an improved diagnostic accuracy in breast lesion characterization compared to MG [1–7]. To date Cu filters with tube voltages within a range of 45–49 kVp were used for the HE images. These settings were used to effectively shape the X-ray spectrum to maximize the proportion of X-rays with energies above the k edge of iodine [22]. Improvements are anticipated to be achievable by combining different levels of tube potentials and target/filter combinations for LE and HE images [16, 23].

In our study, CEDEM was performed using a W anode target and a 1-mm Ti filter at a fixed maximum achievable tube voltage of 49 kVp for the HE images. Previously, these settings led to an increase in the SdNR [9, 13] and the best visibility of iodine in phantom studies [12]. To our knowledge, we are the first to successfully demonstrate the feasibility of this combination in a clinical setting.

All cancers were depicted with CEDEM, including both lesions that were visible or invisible on standard FFDM. All strongly enhancing lesions at CEDEM proved to be carcinomas. Lesions with moderate or no enhancement

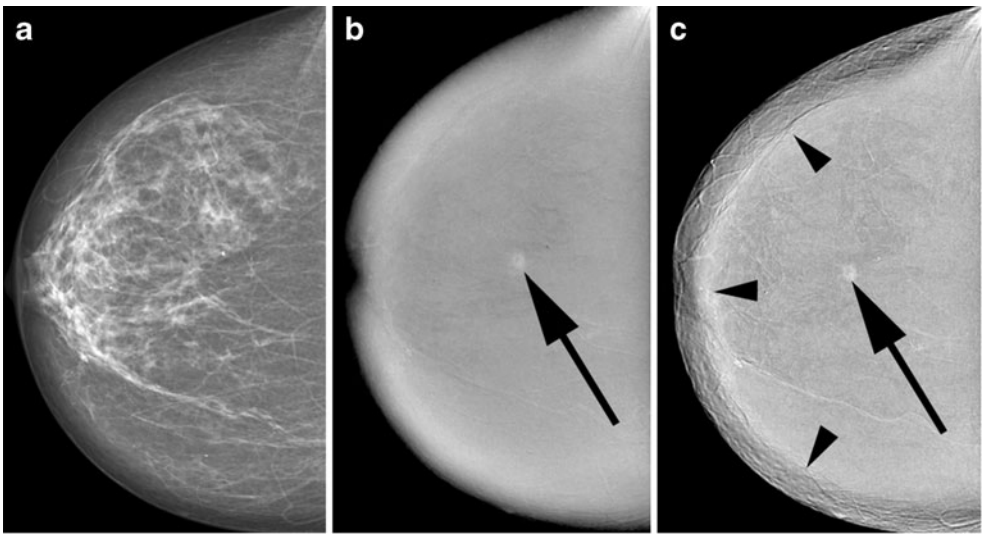

Fig. 2 Mammography (**a**), subtracted contrast-enhanced dual-energy mammography (CEDEM) image with breast thickness-dependent weighting factor (**b**), and with a constant weighting factor (**c**) in a 63-year-old female with an invasive ductal carcinoma (IDC) (arrows in **b** and **c**). A thick rind of increased density surrounding the periphery of the breast is present (arrowheads in **c**) due to over-subtraction. This artefact is overcome when applying a locally dependent weighting factor (**b**)

Table 1 Patient characteristics at mammography (MG) and contrast-enhanced dual-energy mammography (CEDEM)

Patient no.	Pathological finding	Palpable	Breast density (ACR)ε	MG finding	Size* (mm)	MG Shape	CEDEM shape	MG margin	CEDEM margin	CEDEM enhancement	MG BIRADS	CEDEM BIRADS
1	IDC	Yes	A	Mass	40ε	Irregular	Irregular	Spiculated	Spiculated	Strong	5	5
2	IDC	No	A	Mass	8ε	Round	Irregular	Indistinct	Irregular	Strong	4	5
3	Cholesterol granuloma	No	A	Mass	5**	Round		Circumscribed		None	3	2
4	Intraductal papilloma	No	B	Asymmetrical density						None	2	2
5	Fibrocystic change	No	C	Asymmetrical density						None	4	2
6	IDC	No	C	Mass	10ε	Irregular	Irregular	Obscured	Irregular	Strong	4	5
7	IDC	Yes	A	Mass	47ε	Irregular	Irregular	Spiculated	Spiculated	Strong	5	5
8	IDC	No	C	Mass	19ε	Lobular	Irregular	Obscured	Irregular	Strong	4	5
9	IDC #	No	C	Architectural distortion	16/85***		Irregular		Irregular	Strong	4	5
10	IDC §	Yes	C	Mass	64/72***	Round	Irregular	Indistinct	Irregular	Strong	4	4
11	Inflammatory stromal change	Yes	A	Mass	15ε	Irregular	Irregular	Indistinct	Spiculated	Moderate	5	5
12	Fibrocystic change	Yes	C	Architectural distortion	26**					None	4	2
13	Fibrocystic change	No	B	Mass	5**	Lobular		Indistinct		None	4	1
14	IDC §	No	D	Mass	10/69***	Oval	Round	Indistinct	Irregular	Strong	4	5
15	Fibroadenoma	Yes	D	Mass	29ε	Oval	Round	Circumscribed	Smooth	Moderate	3	2

Multifocal cancer

$ Multicentric cancer

* Longest lesion diameter determined at MG and CEDEM

ε Equal for MG and CEDEM

** Only in MG

*** Only in CEDEM

IDC invasive ductal cancer; ACR American College of Radiology

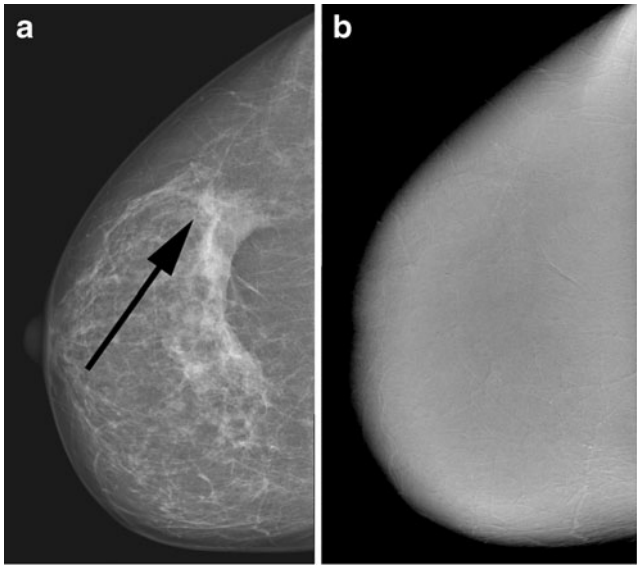

Fig. 3 Mammography (**a**) from a 52-year-old female shows an architectural distortion (arrow in **a**) and was rated as BI-RADS 4. No contrast enhancement is depicted in the suspected region at contrast-enhanced dual-energy mammography (CEDEM), and the lesion was thus rated as BI-RADS 2 (**b**). Histology of the suspected region showed no signs of malignancy

proved to be benign findings at histopathology (Fig. 4). Cancers not visible on FFDM were identified on CEDEM through contrast enhancement, which was especially helpful in radiologically dense breasts. Multifocal and multicentric cancers not detected on MG were depicted on CEDEM.

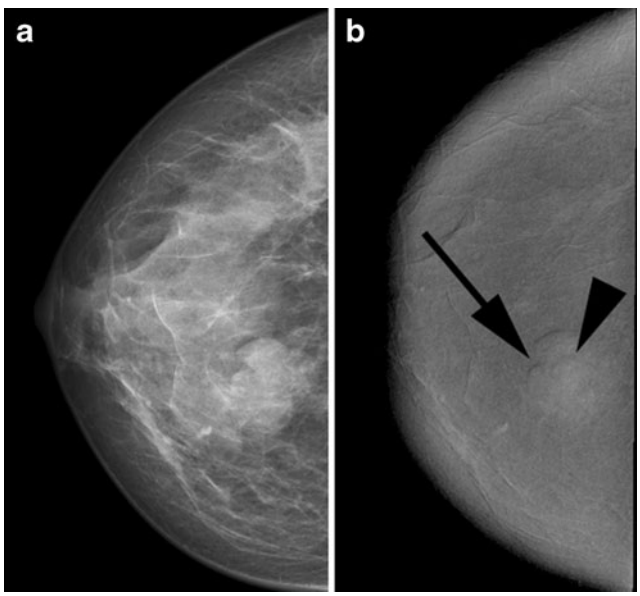

Fig. 4 Mammography (**a**) and subtracted contrast-enhanced dual-energy mammography (CEDEM) image (**b**) of a 47-year-old female with a fibroadenoma. Moderate enhancement is present (**b**) in this benign lesion. Common features of a fibroadenoma can also be depicted in the subtracted CEDEM image with image co-registration and a locally dependent weighting factor for image subtraction: lobulation (arrow in **b**), and thin non-enhancing septa (arrowhead in **b**)

The increase in overall accuracy, especially in dense breasts, the depiction of additional lesions, and a reduction in the false-positive rate is in agreement with other contrast-enhanced MG studies [1, 3, 6].

Post-processing of the acquired HE and LE images is of great importance to allow optimal assessment of the subtracted contrast-enhanced images. We implemented an optimized image subtraction algorithm for CEDEM that has the capability of minimizing the potential of concealing contrast-enhancing lesions at the border of the breast (Fig. 2). However, the effect of this approach needs to be evaluated in direct comparison with post-processing algorithms used in other studies. Jochelson et al. [6], using a simpler image subtraction algorithm, reported that evaluation was limited subsequently in the occurring rind of increased density surrounding the periphery of the breast, and underlines the importance of our endeavour. To avoid motion artefacts, we introduced fully automatic, non-rigid, co-registration of each HE and LE image pair (Fig. 1). This has some impact since it is reported that up to 10 % of examinations had to be excluded due to motion artefacts [24]. This motion can result in a 'black carcinoma', an unexpected decrease in density in the subtracted images, which was explained by the mismatch between the HE and LE image.

A limitation of our study is the small number of patients. The numbers of malignant and benign lesions was not balanced, and thus the breast cancer incidence was much higher compared to the incidence in a screening population. However, this was a feasibility study intended to test a prototype version in a clinical setting. Further research with a larger population is necessary to demonstrate the value of CEDEM using this approach. It can be expected that the results will be at least comparable to other CEDEM systems [1–8].

In conclusion, CEDEM using a Ti filter at a fixed tube voltage of 49 kVp for HE images is feasible. Breast tumours can be analysed with high diagnostic accuracy compared to FFDM. The proposed image-processing algorithm has the potential to reduce artefacts and improve CEDEM images.

Acknowledgments The scientific guarantors of this publication are Thomas H. Helbich, MD. and Thomas Knogler, MD. The authors of this manuscript declare relationships with the following companies: Siemens Healthcare, Erlangen, Germany, and Bracco, Italy. This study has received funding from: Siemens Healthcare, Erlangen, Germany and Bracco, Italy. No complex statistical methods were necessary for this paper. Institutional Review Board approval was obtained. Written informed consent was obtained from all subjects (patients) in this study. Methodology: prospective, experimental, performed at one institution.

References

1. Diekmann F, Freyer M, Diekmann S et al (2011) Evaluation of contrast-enhanced digital mammography. Eur J Radiol 78:112–121
2. Dromain C, Balleyguier C, Adler G, Garbay JR, Delaloge S (2009) Contrast-enhanced digital mammography. Eur J Radiol 69:34–42
3. Dromain C, Thibault F, Diekmann F et al (2012) Dual-energy contrast-enhanced digital mammography: initial clinical results of a multireader, multicase study. Breast Cancer Res BCR 14:R94
4. Jong RA, Yaffe MJ, Skarpathiotakis M et al (2003) Contrast-enhanced digital mammography: initial clinical experience. Radiology 228:842–850
5. Lewin JM, Isaacs PK, Vance V, Larke FJ (2003) Dual-energy contrast-enhanced digital subtraction mammography: feasibility. Radiology 229:261–268
6. Jochelson MS, Dershaw DD, Sung JS et al (2013) Bilateral Contrast-enhanced dual-energy digital mammography: Feasibility and comparison with conventional digital mammography and MR imaging in women with known breast carcinoma. Radiology 266: 743–751
7. Diekmann F, Diekmann S, Jeunehomme F, Muller S, Hamm B, Bick U (2005) Digital mammography using iodine-based contrast media: initial clinical experience with dynamic contrast medium enhancement. Invest Radiol 40:397–404
8. Diekmann F, Bick U (2007) Tomosynthesis and contrast-enhanced digital mammography: recent advances in digital mammography. Eur Radiol 17:3086–3092
9. Hörnig MD, Bätz T, Mertelmeier T (2012) Design of a contrast-enhanced dual-energy tomosynthesis system for breast cancer imaging. Proc SPIE 8313, Medical Imaging 2012: Physics of Medical Imaging 8313
10. Yaffe M (2000) Digital Mammography. In: Beutel J, Kundel HL, Van Metter RL (eds) Handbook of Medical Imaging. SPIE Press, Bellingham
11. Bernhardt P, Mertelmeier T, Hoheisel M (2006) X-ray spectrum optimization of full-field digital mammography: simulation and phantom study. Med Phys 33:4337–4349
12. Samei E, Saunders RS (2011) Dual-energy contrast-enhanced breast tomosynthesis: optimization of beam quality for dose and image quality. Phys Med Biol 56:6359–6378
13. Diekmann F, Sommer A, Lawaczeck R et al (2007) Contrast-to-noise ratios of different elements in digital mammography: evaluation of their potential as new contrast agents. Invest Radiol 42:319–325
14. Carton AK, Gavenonis SC, Currivan JA, Conant EF, Schnall MD, Maidment AD (2010) Dual-energy contrast-enhanced digital breast tomosynthesis—a feasibility study. Br J Radiol 83:344–350
15. Helbich TH (2000) Contrast-enhanced magnetic resonance imaging of the breast. Eur J Radiol 34:208–219
16. Rosado-Mendez I, Palma BA, Brandan ME (2008) Analytical optimization of digital subtraction mammography with contrast medium using a commercial unit. Med Phys 35:5544–5557
17. Rueckert D, Sonoda LI, Hayes C, Hill DL, Leach MO, Hawkes DJ (1999) Nonrigid registration using free-form deformations: application to breast MR images. IEEE Trans Med Imaging 18:712–721
18. Carton AK, Ullberg C, Lindman K, Acciavatti R, Francke T, Maidment AD (2010) Optimization of a dual-energy contrast-enhanced technique for a photon-counting digital breast tomosynthesis system: I. A theoretical model. Med Phys 37: 5896–5907
19. Wallis M, Tardivon A, Helbich T, Schreer I, European Society of Breast I (2007) Guidelines from the European Society of Breast Imaging for diagnostic interventional breast procedures. Eur Radiol 17:581–588
20. Pollard BJ, Samei E, Chawla AS et al (2009) The influence of increased ambient lighting on mass detection in mammograms. Acad Radiol 16:299–304
21. D'Orsi CJ, Sickles EA, Mendelson EB, Morris EA (2013) ACR BI-RADS atlas, breast imaging reporting and data system. American College of Radiology, Reston
22. Skarpathiotakis M, Yaffe MJ, Bloomquist AK et al (2002) Development of contrast digital mammography. Med Phys 29: 2419–2426
23. Leithner R, Knogler T, Homolka P (2013) Development and production of a prototype iodine contrast phantom for CEDEM. Phys Med Biol 58:N25–35
24. Dromain C, Balleyguier C, Muller S et al (2006) Evaluation of tumor angiogenesis of breast carcinoma using contrast-enhanced digital mammography. AJR Am J Roentgenol 187:W528–537